Electronic Research Archive

https://www.aimspress.com/journal/era

ERA, 33(9): 5719–5747.
DOI: 10.3934/era.2025254
Received: 14 June 2025
Revised: 07 September 2025
Accepted: 10 September 2025
Published: 25 September 2025

Research article

On a fractional inverse source problem with mixed boundary conditions through a novel method

Suleyman Cetinkaya*

Department of Mathematics, Kocaeli University, Izmit, Kocaeli 41001, Turkey

* **Correspondence:** Email: suleyman.cetinkaya@kocaeli.edu.tr.

Abstract: In this study, an inverse problem including the identification of a source function in a time-fractional diffusion equation with initial and mixed boundary conditions is investigated by employing the Laplace transform and the Daftardar-Gejji and Jafari method (DJM). Two kinds of inverse problems are considered, where the source function depends either on the temporal variable or the spatial variable. Initially, the Laplace and inverse Laplace transforms are applied to transform the fractional differential equation into an algebraic form. Subsequently, DJM is utilized to establish the solution of the converted problem by using the initial condition. Then, under the mixed boundary conditions, the unknown source function is explicitly determined. The suggested method's ability to obtain the source function under no need for extra conditions and overmeasured data is one of its noteworthy features. The Banach fixed-point theorem and the energy estimate for fractional partial differential equations are also used to theoretically support the existence, uniqueness, and stability of the solution.

Keywords: Daftardar-Gejji and Jafari method; fractional differential equations; inverse source problem; Laplace transformation

1. Introduction

Fractional derivatives are quite useful for modeling a variety of systems in many scientific fields because of their memory and hereditary properties [1, 2]. These characteristics improve their ability to depict intricate physical and engineering phenomena, such as viscoelastic behavior, anomalous diffusion, and procedures found in signal processing, control theory, and bio-engineering [3, 4]. Fractional derivatives provide more realistic depictions of real-world systems by capturing temporal or spatial correlations and non-local dynamics. Fractional partial differential equations (FPDEs) have been addressed through diverse analytical and numerical techniques, including hybrid strategies for the Euler–Bernoulli beam equation [5], homotopy and Elzaki transform methods for nonlinear waves [6], RBF-QR with Gaussian bases [7], Laplace-based series solutions [8], iterative transform methods [9], and wavelet collocation for multi-term FPDEs [10]. Matrix-based frameworks have also been proposed for fractional heat equations [11]. These advancements, pivotal in fields like fluid dynamics, finance, and image processing [12, 13], underscore fractional calculus' interdisciplinary relevance. Among these, the Laplace transform stands out for its ability to simplify FPDEs into algebraic forms, enabling exact or approximate solutions. Recent hybrid approaches leverage it for fractional acoustic waves [14], nonlinear dispersive PDEs [9], coupled time-fractional systems [15], Caputo-type PDEs [16], and other nonlinear/time-fractional models [17–21], highlighting its centrality in FPDE research. A very effective and reliable iterative method for solving nonlinear fractional differential equations in the form of quickly convergent series is the Daftardar-Gejji and Jafari method (DJM). One major benefit of DJM is that, in contrast to conventional perturbation techniques, it does not call for the inclusion of any auxiliary parameters, which streamlines the solution process [22]. Numerous equations, including the Bagley–Torvik and Korteweg–de Vries (KdV) equations, have been successfully solved using this approach [23]. In order to increase accuracy and numerical stability, DJM has also been expanded into hybrid frameworks that include ARA, homotopy analysis, and other integral transformations [24–27]. For a variety of problems, including initial value, boundary value, and integro-differential equations involving both Caputo and Caputo–Fabrizio fractional derivatives, these hybrid approaches allow for derivation of analytical or semi-analytical solutions. The following schematic diagram (Figure 1) illustrates the problem setting:

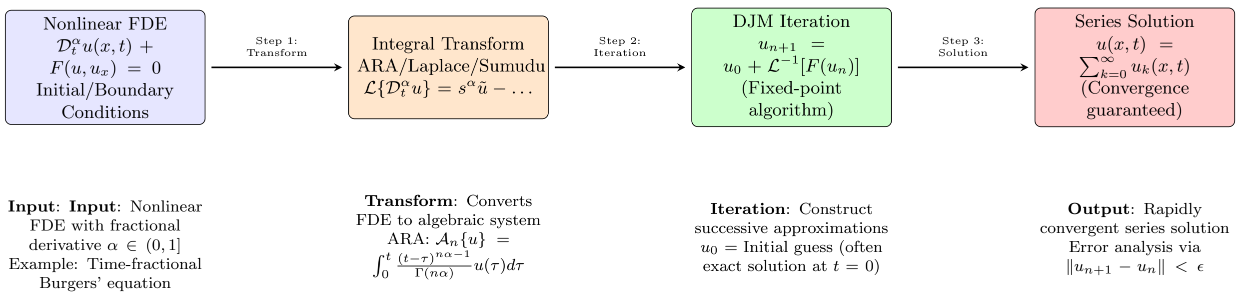

Figure 1. Flowchart of nonlinear fractional differential equation solution via integral transform and DJM.

In many fields, including physics, engineering, hydrology, and biology, inverse source problems are essential for simulating a variety of phenomena. Determining unknown source functions in fractional differential equations greatly improves model fidelity in representing real-world dynamics, which is essential for accurate simulation and prediction. To tackle these issues, a number of analytical and numerical techniques have been developed, such as the generalized Fourier method [28], decomposition methods [29], Rothe-based discretization in conjunction with Galerkin methods [30], regularized minimization strategies [31], sinc wavelet collocation method [32], and the newly defined monic Laguerre wavelets [33]. In this study, we consider the following inverse fractional source problem with initial and mixed boundary conditions:

$$D_t^\alpha u(x,t) = g(x)u_{xx}(x,t) + f, \quad 0 < x < l, \quad 0 < t < T, \quad 0 < \alpha \leq 1,$$
$$u(x,0) = \omega(x),$$

$$u(0,t) = \varphi(t),$$
$$u_x(0,t) = \phi(t),$$

where $g(x)$ represents the diffusion function and f is a function of either the spatial variable x or the time variable t.

We assume $u \in C^{\alpha,3}(\Theta_T)$ where $\Theta_T = \{(x,t) : x \in (0,l), 0 < t \leq T\}$. Here, $C^{\alpha,3}(\Theta_T)$ represents the class of functions that are 3-times continuously differentiable in space whose fractional derivative of order α with respect to t is continuous and whose derivatives up to order 3 are bounded with respect to $x \in (0,l)$. There is a variety of research on the determination of a heat source function which is either space-dependent or time-dependent [34–36].

In order to deal with this problem, we first apply the Laplace transform and inverse Laplace transform to convert the fractional differential equation into an algebraic form. Next, DJM is employed to construct the solution of the transformed problem using the initial condition. Subsequently, the unknown source function is explicitly identified by means of the mixed boundary conditions. The existence, uniqueness, and stability of the solution are demonstrated by using the Banach fixed-point theorem and energy estimates. The analysis of solutions to a class of nonlinear impulsive fractional integro-differential equations of pantograph type was studied in [37,38].

Finally, two examples are given to confirm the efficacy and reliability of the suggested method. The novelty of the proposed method lies in its ability to establish the unknown source function without imposing any additional conditions, unlike existing approaches [39,40]. Furthermore, this method can be readily applied to a wide range of fractional inverse source problems involving different fractional derivatives, demonstrating its broad applicability. Additionally, Laplace transforms and the DJM can be integrated with other techniques to develop more robust and efficient hybrid methods, underscoring the versatility of these approaches.

The objective is to establish a rigorous, innovative, and practically feasible framework for addressing inverse source problems in advanced fractional diffusion models, without relying on excessively restrictive measurement requirements, thereby contributing a significant theoretical and computational methodology with broad applicability in physics, engineering, and finance.

Inverse source problems governed by fractional diffusion equations arise in a wide spectrum of scientific and engineering disciplines due to their ability to capture memory effects, anomalous transport, and non-local interactions. Several representative applications are environmental science and hydrology [41,42], quantitative finance [43,44], and material science and engineering [4,45,46].

The remainder of this paper is structured as follows: Section 2 introduces the fundamental concepts relevant to this study. In Section 3, the fractional inverse source problem for an unknown spatial function is examined and resolved using the proposed method. Section 4 extends the application of this method to the fractional inverse source problem involving an unknown temporal function. The existence, uniqueness, and stability of the solution are analyzed in Section 5. Section 6 presents illustrative examples to validate the obtained results. A comprehensive discussion of the method and its findings is provided in Section 7. Finally, the conclusions are summarized in Section 8.

2. Preliminary results

In this section, preliminaries and fundamental definitions of fractional calculus are presented [2,12].

Definition 1. *Let $u(x,t)$ be a real valued function. Its Riemann-Liouville time fractional integral of order $\alpha > 0$ is denoted by $\mathcal{I}_t^{\alpha} u(x,t)$, and is defined as*

$$\mathcal{I}_t^{\alpha} u(x,t) = \frac{1}{\Gamma(\alpha)} \int_0^t \frac{u(x,s)}{(t-s)^{1-\alpha}}\, ds,$$

where the Euler gamma function $\Gamma(\alpha)$ is defined by

$$\Gamma(\alpha) = \int_0^{\infty} e^{-t} t^{\alpha-1}\, dt, \quad \mathrm{Re}(\alpha) > 0.$$

Definition 2. *The definition of the Caputo time fractional derivative of $u(x,t)$ is given as*

$$\mathcal{D}_t^{\alpha} u(x,t) = \begin{cases} \dfrac{1}{\Gamma(n-\alpha)} \displaystyle\int_0^t \frac{\partial^n}{\partial s^n} u(x,s)(t-s)^{n-\alpha-1} ds, & n-1 < \alpha < n, \\ \dfrac{\partial^n}{\partial t^n} u(x,t), & \alpha = n, \end{cases}$$

where $n \in \mathbb{N}$.

Definition 3. *The incomplete gamma functions are defined by the integrals*

$$\gamma(a,z) = \int_0^z t^{a-1} e^{-t}\, dt,$$

$$\Gamma(a,z) = \int_z^{\infty} t^{a-1} e^{-t}\, dt,$$

where the integration pathways do not cross the negative real axis, and α and t are complex variables. The constraint $\mathrm{Re}(\alpha) > 0$ is necessary for the definition of $\gamma(a,z)$, whereas $|\arg(z)| < \pi$ is assumed for $\Gamma(a,z)$ [47].

Definition 4. *The definition of the Mittag-Leffler function of two parameters $E_{\alpha,\beta}(x)$ is given as*

$$E_{\alpha,\beta}(x) = \sum_{j=0}^{\infty} \frac{x^j}{\Gamma(\alpha j + \beta)},$$

where $\mathrm{Re}(\alpha) > 0$, $x, \beta \in \mathbb{C}$.

Definition 5. *The Laplace transformation is defined as [48, 49]*

$$\mathcal{L}[f(t)](s) = F(s) = \int_0^{\infty} e^{-st} f(t)\, dt,$$

which exists for the following set of piecewise continuous functions:

$$\left\{ f(t) : \exists M, k > 0, \text{ such that } |f(t)| < M e^{k\tau}, \tau \in [0,\infty) \right\}.$$

Property 1.

$$\mathcal{L}\left[\frac{t^{n\alpha}}{\Gamma(n\alpha+1)}\right](s) = \frac{1}{s^{n\alpha+1}}; \quad n, \alpha > 0$$

is a significant property used in this research. Moreover, the inverse Laplace transformation of it is obtained as

$$\mathcal{L}^{-1}\left[\frac{1}{s^{n\alpha+1}}\right](t) = \frac{t^{n\alpha}}{\Gamma(n\alpha+1)}, \quad \mathrm{Re}(\alpha) > 0.$$

Property 2. *The Laplace transformation for the Caputo time fractional derivative of two variable functions $u(x,t)$ is given as*

$$\mathcal{L}\left[\mathcal{D}_t^{\alpha} u(x,t)\right](s) = s^{\alpha}\mathcal{L}[u(x,t)](s) - \sum_{j=0}^{n-1} s^{\alpha-j-1}\frac{\partial^j}{\partial t^j}u(x,0),$$

where $n-1 < \alpha \leq n$, $n \in \mathbb{N}$.

Definition 6. *The convolution of two functions $f(t)$ and $g(t)$ defined on $[0,\infty)$ is defined as*

$$(f * g)(t) = \int_0^t f(t-\tau)g(\tau)\,d\tau = \int_0^t f(\tau)g(t-\tau)\,d\tau,$$

provided the integral exists for all $t \geq 0$ [50].

Property 3. *The product of the Laplace transforms of the two functions is the Laplace transform of the convolution of the two functions:*

$$\mathcal{L}[(f * g)(t)](s) = \mathcal{L}[f(t)](s) \cdot \mathcal{L}[g(t)](s), \quad s > s_0.$$

Lemma 1. *Let $f : [a,b] \to \mathbb{R}$ be a function such that $\mathcal{D}_x^{k\alpha} f(x) \in C(a,b]$ for $k = 0,1,2,\ldots,n+1$ where $0 < \alpha \leq 1$. Then, its fractional Taylor expansion is given as [51]*

$$f(x) \cong P_N^{\alpha}(x) = \sum_{i=0}^{N} \frac{(x-a)^{i\alpha}}{\Gamma(i\alpha+1)}\left(\mathcal{D}_a^{i\alpha} f\right)(a) + R_N^{\alpha}(x),$$

where the remainder term is

$$R_N^{\alpha}(x) = \frac{\left(\mathcal{D}_a^{(N+1)\alpha} f\right)(\xi)}{\Gamma((N+1)\alpha+1)}(x-a)^{(N+1)\alpha},$$

for some $\xi \in (a,x)$.

3. Fractional inverse source problem with unknown function of spatial variable x

In this section, we consider the following fractional inverse source problem:

$$\mathcal{D}_t^{\alpha} u(x,t) = g(x)u_{xx}(x,t) + f(x), \qquad x > 0,\ 0 < \alpha \leq 1,\ 0 < t < T, \tag{3.1}$$

$$u(x,0) = \omega(x), \tag{3.2}$$

$$u(0,t) = \varphi(t), \tag{3.3}$$
$$u_x(0,t) = \phi(t), \tag{3.4}$$

where $f(x)$ could denote heat source distribution spatially along an object.

The algorithm of the proposed method includes the following steps:

Step 1: Application of Laplace transformation to Eq (3.1) yields

$$U(x,s) = \frac{1}{s}u(x,0) + \frac{1}{s^{\alpha}}\mathcal{L}\left[g(x)u_{xx}(x,t) + f(x)\right](s). \tag{3.5}$$

Step 2: Application of inverse Laplace transform to Eq (3.5) and Property 1 leads to

$$u(x,t) = \mathcal{L}^{-1}\left[\frac{1}{s}u(x,0)\right] + \mathcal{L}^{-1}\left[\frac{1}{s^{\alpha}}\mathcal{L}\left[g(x)u_{xx}(x,t) + f(x)\right](s)\right].$$

Step 3: Utilization of DJM provides the solution in the following form:

$$u(x,t;\alpha) = u_0(x,t) + \sum_{k=1}^{\infty} u_k(x,t;\alpha),$$

where $u_0(x,t)$ is computed as

$$u_0(x,t) = \mathcal{L}^{-1}\left[\frac{1}{s}u(x,0)\right] = \omega(x).$$

Step 4: The formula for $u_1(x,t;\alpha)$ is obtained as

$$u_1(x,t;\alpha) = \mathcal{L}^{-1}\left[\frac{1}{s^{\alpha}}\mathcal{L}\left[g(x)(u_0(x,t))_{xx} + f(x)\right](s)\right].$$

Step 5: The formula for $u_n(x,t;\alpha)$ for $n \geq 2$ is established as

$$\begin{aligned} u_n(x,t;\alpha) = {} & \mathcal{L}^{-1}\left[\frac{1}{s^{\alpha}}\mathcal{L}\left[g(x)\left(\sum_{k=0}^{n-1} u_k(x,t)\right)_{xx} + f(x)\right](s)\right] \\ & - \mathcal{L}^{-1}\left[\frac{1}{s^{\alpha}}\mathcal{L}\left[g(x)\left(\sum_{k=0}^{n-2} u_k(x,t)\right)_{xx} + f(x)\right](s)\right]. \end{aligned}$$

Step 6: The truncated solution is acquired in the series form as

$$u(x,t;\alpha) = u_0(x,t) + \sum_{k=1}^{n} u_k(x,t;\alpha). \tag{3.6}$$

Step 7: Utilization of boundary conditions (3.3) and (3.4) together with Eq (3.6) yields the unknown source function $f(x)$.

The following flowchart in Figure 2 illustrates the framework of the proposed method for the identification of the unknown function of spatial variable x:

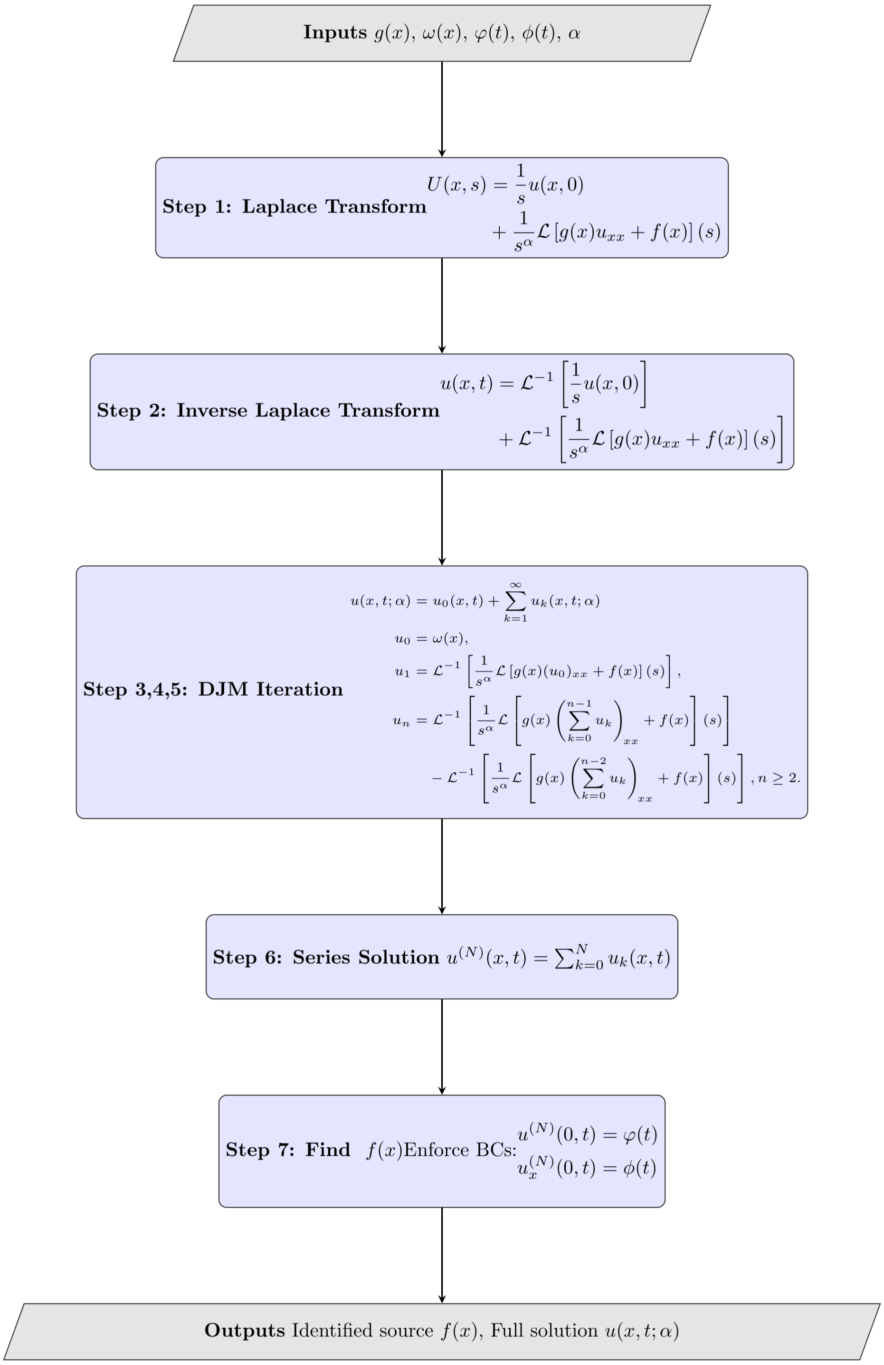

Figure 2. Fractional inverse source problem with unknown function of spatial variable x.

4. Fractional inverse source problem with unknown function of time variable t

Consider the following fractional inverse source problem:

$$\mathcal{D}_t^\alpha u(x,t) = g(x)u_{xx}(x,t) + f(t), \qquad 0 < x < l,\ 0 < t < T,\ 0 < \alpha \leq 1, \tag{4.1}$$

$$u(x,0) = \omega(x), \tag{4.2}$$
$$u(0,t) = \varphi(t), \tag{4.3}$$
$$u_x(0,t) = \phi(t), \tag{4.4}$$

where $f(t)$ could denote heat source distribution in time along an object.

The algorithm of the proposed method takes the following steps:

Step 1: Applying the Laplace transform to Eq (4.1) gives rise to the following:

$$U(x,s) = \frac{1}{s}u(x,0) + \frac{1}{s^{\alpha}}\mathcal{L}\left[g(x)u_{xx}(x,t) + f(t)\right](s). \tag{4.5}$$

Step 2: Applying the inverse Laplace transform to Eq (4.5) and Property 1 leads to

$$u(x,t) = \mathcal{L}^{-1}\left[\frac{1}{s}u(x,0)\right] + \mathcal{L}^{-1}\left[\frac{1}{s^{\alpha}}\mathcal{L}\left[g(x)u_{xx}(x,t) + f(t)\right](s)\right].$$

Step 3: DJM provides the solution in series form as

$$u(x,t;\alpha) = u_0(x,t) + \sum_{k=1}^{\infty} u_k(x,t;\alpha),$$

where

$$u_0(x,t) = \mathcal{L}^{-1}\left[\frac{1}{s}u(x,0)\right] = \omega(x).$$

Step 4: $u_1(x,t;\alpha)$ is obtained as

$$u_1(x,t;\alpha) = \mathcal{L}^{-1}\left[\frac{1}{s^{\alpha}}\mathcal{L}\left[g(x)\left(u_0(x,t)\right)_{xx}\right](s)\right] + \mathcal{L}^{-1}\left[\frac{1}{s^{\alpha}}\mathcal{L}\left[f(t)\right](s)\right].$$

Rearrangement of the above expression yields

$$u_1(x,t;\alpha) = \mathcal{L}^{-1}\left[\frac{1}{s^{\alpha}}\mathcal{L}\left[g(x)\left(u_0(x,t)\right)_{xx}\right](s)\right] + \left(\frac{t^{\alpha-1}}{\Gamma(\alpha)} * f(t)\right). \tag{4.6}$$

Step 5: $u_n(x,t;\alpha)$ for $n \geq 2$ is acquired by DJM as

$$u_n(x,t;\alpha) = \mathcal{L}^{-1}\left[\frac{1}{s^{\alpha}}\mathcal{L}\left[g(x)\left(\sum_{k=0}^{n-1} u_k(x,t)\right)_{xx} + f(t)\right](s)\right] - \mathcal{L}^{-1}\left[\frac{1}{s^{\alpha}}\mathcal{L}\left[g(x)\left(\sum_{k=0}^{n-2} u_k(x,t)\right)_{xx} + f(t)\right](s)\right].$$

Step 6: The truncated solution is obtained as

$$u(x,t;\alpha) = u_0(x,t) + \sum_{k=1}^{n} u_k(x,t;\alpha). \tag{4.7}$$

Step 7: Using the boundary condition (4.3) and Eq (4.7) provides the solution for unknown source function.

Notice that the boundary condition (4.4) is not utilized in the determination of the unknown source function $f(t)$ unlike $f(x)$.

The following flowchart in Figure 3 illustrates the framework of the proposed method for the identification of the unknown function of time variable t:

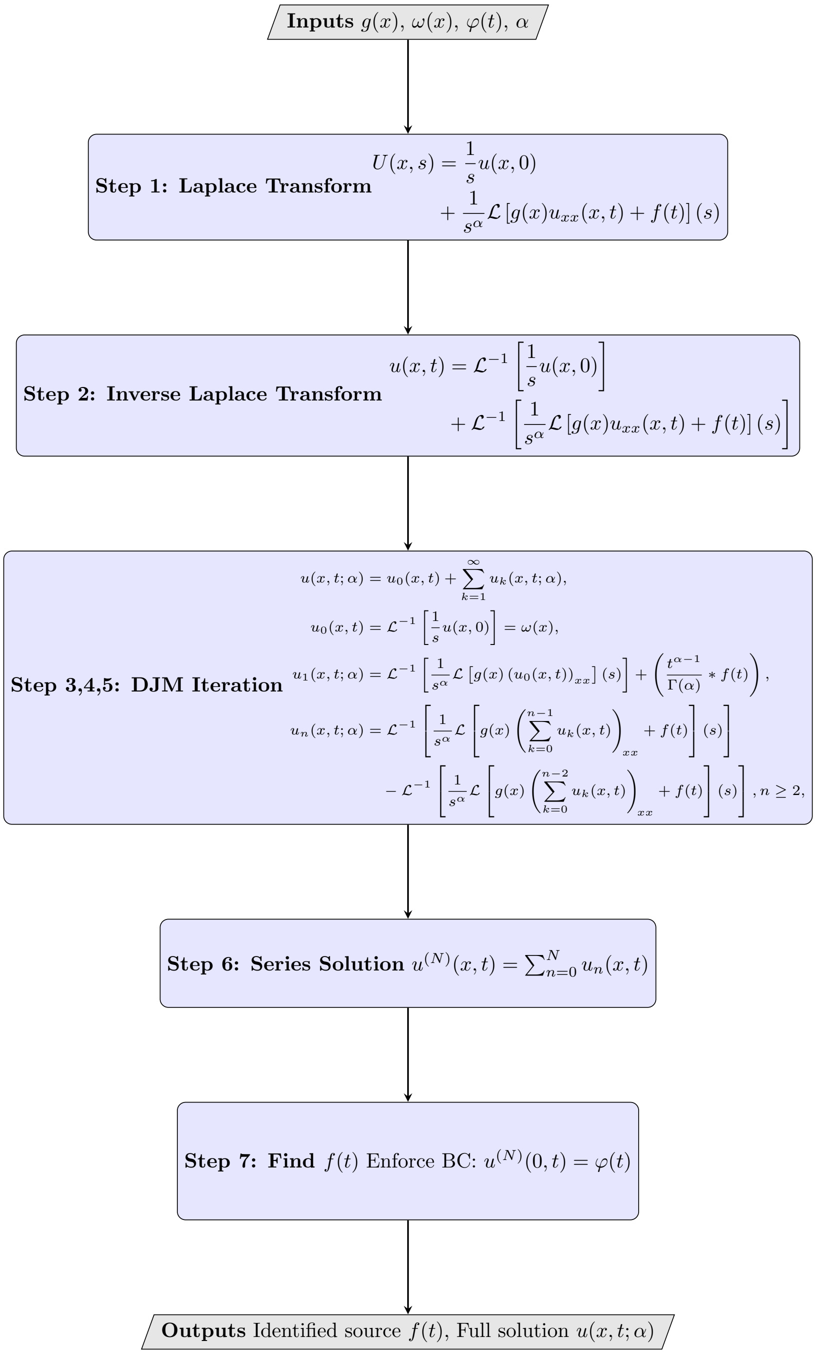

Figure 3. Fractional inverse source problem with unknown function of time variable t.

5. Existence, uniqueness, and stability of the fractional inverse source problems

5.1. Existence, uniqueness, and stability of the fractional inverse source problem of spatial variable x

The following theorems assert the uniqueness and the stability of the inverse problems (3.1)–(3.4) in which $H^{\alpha}(\mathbb{R})$ represents the class of locally Hölder continuous functions with exponent $\alpha \in (0,1)$. Moreover, the norm of the Hölder space $C^{1,\alpha}$ is defined as

$$\|u\|_{C^{1,\alpha}} := \sup|u| + \sup|u'| + \sup_{x\neq y}\frac{|u'(x)-u'(y)|}{|x-y|^{\alpha}}.$$

Theorem 1 (Existence and Uniqueness). *If* $g(x) \in C^{1,\alpha}([0,l])$, $\omega(x) \in H^{\alpha+3}((0,l))$, $\varphi(t) \in C^{1,\alpha}([0,T])$, $\phi(t) \in C^{1,\alpha}([0,T])$, $\|\omega\|_{H^{\alpha+3}} \geq v_0 > 0$, $\|\phi\|_{C^{1,\alpha}} \geq v_1 > 0$, *and* $\|\varphi\|_{C^{1,\alpha}} \geq v_2 > 0$ *with* $\omega(0) = u(0,0) = \varphi(0)$, *then there exists a number* $l_1 \in (0,l)$ *such that there exists a unique solution* $f(x) \in C^{1,\alpha}([0,l_1])$ *of the inverse problems (3.1)–(3.4).*

Proof. Taking the Riemann-Liouville integral of Eq (3.1) with respect to time yields

$$u(x,t) = \omega(x) + \frac{1}{\Gamma(\alpha)}\int_0^t (t-s)^{\alpha-1}\left[g(x)u_{xx}(x,s) + f(x)\right]ds. \tag{5.1}$$

The boundary condition at $x = 0$ is obtained as

$$\varphi(t) = \omega(0) + \frac{1}{\Gamma(\alpha)}\int_0^t (t-s)^{\alpha-1}\left[g(0)u_{xx}(0,s) + f(0)\right]ds.$$

Taking the derivative with respect to t leads to the following Volterra type equation for $u_{xx}(0,t)$:

$$\varphi'(t) = \frac{g(0)}{\Gamma(\alpha)}\frac{d}{dt}\int_0^t (t-s)^{\alpha-1}u_{xx}(0,s)ds + \frac{f(0)}{\Gamma(\alpha)}\frac{d}{dt}\int_0^t (t-s)^{\alpha-1}ds,$$

which allows us to recover $f(0)$ uniquely.

Similarly, taking the derivative of (5.1) with respect to x yields

$$u_x(x,t) = \omega'(x) + \frac{1}{\Gamma(\alpha)}\int_0^t (t-s)^{\alpha-1}\left[g'(x)u_{xx}(x,s) + g(x)u_{xxx}(x,s) + f'(x)\right]ds.$$

The second boundary condition at $x = 0$ is obtained as

$$\phi(t) = \omega'(0) + \frac{1}{\Gamma(\alpha)}\int_0^t (t-s)^{\alpha-1}\left[g'(0)u_{xx}(0,s) + g(0)u_{xxx}(0,s) + f'(0)\right]ds.$$

Taking the derivative with respect to t leads to the following Volterra type equation for $u_{xxx}(0,t)$:

$$\phi'(t) = \frac{1}{\Gamma(\alpha)}\frac{d}{dt}\int_0^t (t-s)^{\alpha-1}\left[g'(0)u_{xx}(0,s) + g(0)u_{xxx}(0,s) + f'(0)\right]ds.$$

Substituting the obtained $u_{xx}(0,t)$ into the above equation leads to the unique determination of $f'(0)$.

Now let us define the following linear operator which maps $C([0,l_1])$ into itself for sufficiently small l_1, acting on $f(x)$ as

$$\mathcal{M}f(x) = \mathcal{D}_t^{\alpha}u(x,t) - g(x)u_{xx}(x,t),$$

where $u(x,t)$ represents the solution of the problems (3.1)–(3.4).

The Lipschitz continuity of $g(x)$ and the boundedness of $\omega(x)$, $\varphi(t)$, and $\phi(t)$ imply the contraction of the operator with the help of the Banach fixed-point theorem. As a result, we obtain

$$\|\mathcal{M}f_1 - \mathcal{M}f_2\| \le Cl_1^{\alpha}\|f_1 - f_2\|_{C^{1,\alpha}},$$

from

$$\|u_{xx}(\cdot; f_1) - u_{xx}(\cdot; f_2)\|_{C^{\alpha}} \le L\|f_1 - f_2\|_{C^{1,\alpha}},$$

where C depends on g, ω, φ, and ϕ, and L is a constant.

The combination of Volterra equations with Lipschitz continuity yields

$$|f_1(0) - f_2(0)| \le \|\varphi_1' - \varphi_2'\|_{C^{\alpha}} + g(0)L\|\omega_1 - \omega_2\|_{H^{\alpha+3}},$$

which can be extended to $\|f_1 - f_2\|_{C^{1,\alpha}}$ by means of integral estimates.

Taking l_1 small enough guarantees that $Cl_1^{\alpha} < 1$, which implies the uniqueness of the solution $f(x)$ in $C^1([0, l_1])$.

The set $\Lambda(\sigma_0)$ includes the functions $(f, \omega, \varphi, \phi)$ which satisfy the conditions of Theorem 1 so that

$$\max\{\|\omega\|_{H^{\alpha+3}}, \|\varphi\|_{C^{1,\alpha}}, \|\phi\|_{C^{1,\alpha}}, \|f\|_{C^{1,\alpha}}\} \le \sigma_0.$$

Moreover, $\Psi(\sigma_1)$, $\Psi(\sigma_2)$, and $\Psi(\sigma_3)$ denote

- the set of functions $f(x) \in C^{1,\alpha}([0, l_1])$ satisfying the inequality $\|f\|_{C^{1,\alpha}} \le \sigma_1$,
- the set of functions $\varphi(t) \in C^{1,\alpha}([0, T])$ satisfying the inequality $\|\varphi\|_{C^{1,\alpha}} \le \sigma_2$,
- the set of functions $\phi(t) \in C^{1,\alpha}([0, T])$ satisfying the inequality $\|\phi\|_{C^{1,\alpha}} \le \sigma_3$,

respectively.

Theorem 2 (Stability). *Let $(f_1, \omega_1, \varphi_1, \phi_1) \in \Lambda(\sigma_0)$, $(f_2, \omega_2, \varphi_2, \phi_2) \in \Lambda(\sigma_0)$ with $(f_1, f_2) \in \Psi(\sigma_1)$, $(\varphi_1, \varphi_2) \in \Psi(\sigma_2)$, and $(\phi_1, \phi_2) \in \Psi(\sigma_3)$. Then, the solution of the inverse problems (3.1)–(3.4) satisfies the following stability estimate:*

$$\|f_1(x) - f_2(x)\|_{C^{1,\alpha}} \le C_1\left(\|\omega_1(x) - \omega_2(x)\|_{H^{\alpha+3}} + \|\varphi_1(x) - \varphi_2(x)\|_{C^{1,\alpha}} + \|\phi_1(x) - \phi_2(x)\|_{C^{1,\alpha}}\right),$$

where the constant C_1 depends on l, α, σ_0, σ_1, σ_2, and σ_3.

Proof. The proof follows from the inequality

$$|f_1(x) - f_2(x)| \le |\mathcal{D}_t^{\alpha}(u_1 - u_2)| + |g(x)||(u_1)_{xx} - (u_2)_{xx}|$$

and the energy estimates for the partial differential equation.

5.2. Existence, uniqueness, and stability of the fractional inverse source problem of time variable t

Theorem 3 (Existence and Uniqueness). *If $g(x) \in C^{1,\alpha}([0, l])$, $\omega(x) \in H^{\alpha+2}((0, l))$, $\varphi(t) \in C^{1,\alpha}([0, T])$, $\phi(t) \in C^{1,\alpha}([0, T])$, with $\|\omega\|_{H^{\alpha+2}} \ge v_0 > 0$, $\|\phi\|_{C^{1,\alpha}} \ge v_1 > 0$, $\omega(0) = u(0, 0) = \varphi(0)$, and $g(x) \ge c > 0$ for some constant c, then there exists $T_1 \in (0, T)$ such that there exists a unique solution $f(t) \in C([0, T_1])$ of the inverse problems (4.1)–(4.4).*

Proof. Taking the Riemann-Liouville integral of order α of Eq (4.1) yields the following Volterra-type equation:

$$u(x,t) = \omega(x) + \mathcal{I}_t^\alpha \left(g(x)u_{xx}(x,t) + f(t)\right).$$

Employing boundary condition (4.3) provides

$$\varphi(t) = \omega(0) + \frac{1}{\Gamma(\alpha)} \int_0^t (t-s)^{\alpha-1} \left[g(0)u_{xx}(0,s) + f(s)\right] ds. \tag{5.2}$$

Solving (5.2) for $f(t)$ leads to

$$f(t) = \mathcal{D}_t^\alpha \varphi(t) - g(0)u_{xx}(0,t). \tag{5.3}$$

Therefore, utilizing (5.3), we define the following map for the uniqueness of the solution:

$$G(f)(t) = \mathcal{D}_t^\alpha \varphi(t) - g(0)u_{xx}(0,t;f),$$

whose contraction on $C([0,T_1])$ for some $T_1 < T$ can be proved as follows.

Exploiting energy estimates for fractional PDEs gives

$$\|u_{xx}(0,t)\|_{C([0,T])} \leq P\left(\|\omega\|_{H^{\alpha+2}} + \|\varphi\|_{C^{1,\alpha}} + \|\phi\|_{C^{1,\alpha}} + \|f\|_{C([0,T])}\right),$$

which implies the Lipschitz continuity of the direct problem solution with respect to f:

$$\|u_{xx}(0,t;f_1) - u_{xx}(0,t;f_2)\|_{C([0,T])} \leq LT^\alpha \|f_1 - f_2\|_{C([0,T])}. \tag{5.4}$$

Its derivation relies on the representation of the solution through a Volterra-type integral operator with kernel $K(x,t)$, whose regularity properties are well established in the literature [52]

More precisely, the difference $w = u_1 - u_2$ satisfies a homogeneous equation with source term $\tilde{f} = f_1 - f_2$. Employing the integral representation and the key property

$$|\partial_{xx}K(0,t)| \leq Ct^{\alpha-1},$$

which governs the behavior of the second derivative of the kernel, we obtain

$$|w_{xx}(0,t)| \leq C\|f_1 - f_2\|_{C([0,T])} \int_0^t (t-s)^{\alpha-1} s^{\alpha-1}\, ds \leq LT^\alpha \|f_1 - f_2\|_{C([0,T])}.$$

For two prospective source functions f_1 and f_2, the difference $G(f_1)(t) - G(f_2)(t)$ satisfies

$$|G(f_1)(t) - G(f_2)(t)| \leq g(0)|u_{xx}(0,t;f_1) - u_{xx}(0,t;f_2)|.$$

Making use of (5.4) gives rise to the following contraction condition:

$$\|G(f_1) - G(f_2)\|_{C([0,T_1])} \leq g(0)LT_1^\alpha \|f_1 - f_2\|_{C([0,T_1])},$$

for suitable T_1 such that $g(0)LT_1^\alpha < 1$.

The stability bound for perturbations in data is provided by the following:

$$\|f_1 - f_2\|_{C([0,T_1])} \leq \|\mathcal{D}_t^\alpha \varphi_1 - \mathcal{D}_t^\alpha \varphi_2\|_{C([0,T_1])} + g(0)LT_1^\alpha \|\omega_1 - \omega_2\|_{H^{\alpha+2}}.$$

Since $C([0,T_1])$ is a Banach space, the Banach fixed-point theorem indicates that there exists a unique solution $f(t) \in C([0,T_1])$ of the inverse problem.

Theorem 4 (Stability)**.** *Let $f_1(t)$ and $f_2(t)$ be solutions of the inverse problems (4.1)–(4.4) corresponding to the data $(\varphi_1, \phi_1, \omega_1)$ and $(\varphi_2, \phi_2, \omega_2)$, respectively. Assume:*

1) $g(x) \in C([0, l])$ with $g(x) \geq g_0 > 0$,

2) $\omega_1, \omega_2 \in H^{\alpha+2}((0, l))$, $\varphi_1, \varphi_2 \in C^{1,\alpha}([0, T])$, $\phi_1, \phi_2 \in C^{1,\alpha}([0, T])$,

3) the direct problem for $u(x, t; f)$ is well-posed with Lipschitz dependence on f.

Then, the following stability estimate holds:

$$\|f_1 - f_2\|_{C([0,T_1])} \leq R\left(\|\varphi_1 - \varphi_2\|_{C^{1,\alpha}([0,T])} + \|\phi_1 - \phi_2\|_{C^{1,\alpha}([0,T])} + \|\omega_1 - \omega_2\|_{H^{\alpha+2}((0,l))}\right),$$

where R depends on g_0, T_1, α, and the norms of the input data.

Proof. From (5.3), we have

$$\|f_1 - f_2\|_{C([0,T_1])} \leq \|\mathcal{D}_t^\alpha \varphi_1 - \mathcal{D}_t^\alpha \varphi_2\|_{C^\alpha([0,T_1])} + g_0\|u_{xx}^1(0, t) - u_{xx}^2(0, t)\|_{C([0,T_1])}. \tag{5.5}$$

Since $\varphi_1, \varphi_2 \in C^{1,\alpha}([0, T])$, the Caputo derivative $\mathcal{D}_t^\alpha$ satisfies

$$\|\mathcal{D}_t^\alpha \varphi_1 - \mathcal{D}_t^\alpha \varphi_2\|_{C^\alpha([0,T_1])} \leq P_\alpha\|\varphi_1 - \varphi_2\|_{C^{1,\alpha}([0,T])}.$$

From the fact that the solution to the direct problem is Lipschitz continuous and from energy estimates, we get

$$\|u_{xx}^1(0, t) - u_{xx}^2(0, t)\|_{C([0,T_1])} \leq L\left(\|\omega_1 - \omega_2\|_{H^{\alpha+2}} + \|\varphi_1 - \varphi_2\|_{C^{1,\alpha}} + \|\phi_1 - \phi_2\|_{C^{1,\alpha}}\right).$$

These results lead (5.5) to the following inequality:

$$\|f_1 - f_2\|_{C([0,T_1])} \leq P_\alpha\|\varphi_1 - \varphi_2\|_{C^{1,\alpha}} + g_0 L\left(\|\omega_1 - \omega_2\|_{H^{\alpha+2}} + \|\varphi_1 - \varphi_2\|_{C^{1,\alpha}} + \|\phi_1 - \phi_2\|_{C^{1,\alpha}}\right).$$

Defining $P = \max\{P_\alpha, g(0)L\}$, we have

$$\|f_1 - f_2\|_{C([0,T_1])} \leq P\left(\|\omega_1 - \omega_2\|_{H^{\alpha+2}} + \|\varphi_1 - \varphi_2\|_{C^{1,\alpha}} + \|\phi_1 - \phi_2\|_{C^{1,\alpha}}\right).$$

6. Demonstrative examples

Two examples are provided to present the implementation of the algorithms for the proposed method and to verify the effectiveness and accuracy of it. Example 1 can be considered as a mathematical model of drug diffusion with drug release rate of $f(x)$ as well as contaminant plume with an unknown pollutant source function $f(x)$. The Example 2 can be utilized to model thermal processes with time-varying heat input $f(t)$ as well as reaction-diffusion systems with a time-dependent reactant injection rate $f(t)$.

Example 1. *Consider the fractional inverse source problem*

$$\mathcal{D}_t^\alpha u(x, t) = 2u_{xx}(x, t) + f(x), \qquad x > 0,\ 0 < \alpha \leq 1,\ t > 0, \tag{6.1}$$

$$u(x, 0) = e^x + \sin(x), \tag{6.2}$$

$$u(0,t) = e^{2t}, \tag{6.3}$$
$$u_x(0,t) = e^{2t} + 1. \tag{6.4}$$

where $u(x,t)$ represents the concentration of a diffusing substance (e.g., a solute, pollutant, or thermal energy) at position $x > 0$ and time $t > 0$. The constant diffusion coefficient is 2, and $f(x)$ denotes a time-invariant source (or sink) term distributed spatially within the medium.

The inverse problem consists of determining the unknown spatial source function $f(x)$ from the given boundary and initial data. This finds practical application in several fields, including:

- ***Hydrology**: Identifying contaminant sources in groundwater systems.*
- ***Bioengineering**: Reconstructing internal source distributions in tissues from surface measurements.*
- ***Non-destructive Testing**: Detecting hidden defects or sources in materials through boundary sensor data.*

Application of Laplace and inverse Laplace transforms to Eq (6.1) successively yields:

$$u(x,t) = \mathcal{L}^{-1}\left[\frac{1}{s}\left(e^x + \sin(x)\right)\right] + \mathcal{L}^{-1}\left[\frac{1}{s^\alpha}\mathcal{L}\left[2u_{xx}(x,t) + f(x)\right](s)\right].$$

Here, $u_0(x,t)$ is formulated as follows:

$$u_0(x,t) = e^x + \sin(x).$$

$u_1(x,t;\alpha)$ is obtained by DJM as

$$u_1(x,t;\alpha) = \frac{t^\alpha}{\Gamma(\alpha+1)}\left[2\left(e^x - \sin(x)\right) + f(x)\right].$$

Similarly, $u_2(x,t;\alpha)$ and $u_3(x,t;\alpha)$ are obtained by DJM as

$$u_2(x,t;\alpha) = 2\frac{t^{2\alpha}}{\Gamma(2\alpha+1)}\left[2\left(e^x + \sin(x)\right) + f''(x)\right],$$
$$u_3(x,t;\alpha) = 2\left(2\frac{t^{3\alpha}}{\Gamma(3\alpha+1)}\left[2\left(e^x - \sin(x)\right) + f^{(4)}(x)\right]\right).$$

The truncated solution is established as

$$\begin{aligned} u(x,t;\alpha) &= e^x\left(1 + 2\frac{t^\alpha}{\Gamma(\alpha+1)} + 4\frac{t^{2\alpha}}{\Gamma(2\alpha+1)} + 8\frac{t^{3\alpha}}{\Gamma(3\alpha+1)} + \cdots\right) \\ &\quad + \sin(x)\left(1 - 2\frac{t^\alpha}{\Gamma(\alpha+1)} + 4\frac{t^{2\alpha}}{\Gamma(2\alpha+1)} - 8\frac{t^{3\alpha}}{\Gamma(3\alpha+1)} + \cdots\right) \\ &\quad + f(x)\frac{t^\alpha}{\Gamma(\alpha+1)} + 2f''(x)\frac{t^{2\alpha}}{\Gamma(2\alpha+1)} + 4f^{(4)}(x)\frac{t^{3\alpha}}{\Gamma(3\alpha+1)} + \cdots \\ &= e^x E_{\alpha,1}(2t^\alpha) + \sin(x)E_{\alpha,1}(-2t^\alpha) \\ &\quad + f(x)\frac{t^\alpha}{\Gamma(\alpha+1)} + 2f''(x)\frac{t^{2\alpha}}{\Gamma(2\alpha+1)} + 4f^{(4)}(x)\frac{t^{3\alpha}}{\Gamma(3\alpha+1)} + \cdots. \end{aligned} \tag{6.5}$$

Utilizing boundary condition (6.3), we get $u(0,t;\alpha) = u(0,t)$*, i.e.,*

$$\begin{aligned} e^{2t} = 1 &+ \frac{t^{\alpha}}{\Gamma(\alpha+1)}\left(2 + f(0)\right) + \frac{t^{2\alpha}}{\Gamma(2\alpha+1)}\left(4 + 2f''(0)\right) \\ &+ \frac{t^{3\alpha}}{\Gamma(3\alpha+1)}\left(8 + 4f^{(4)}(0)\right) + \cdots . \end{aligned}$$

So, the fractional Taylor series expansion of $e^{2t} = \sum_{k=0}^{\infty} \frac{t^{k\alpha}}{\Gamma(k\alpha+1)} 2^{k\alpha}$ *at* $t = 0$ *leads to*

$$f^{(2n)}(0;\alpha) = \frac{(2^{n+1})^{\alpha} - 2^{n+1}}{2^n}, \quad n = 0, 1, 2, \cdots . \tag{6.6}$$

Employing boundary condition (6.4), we have

$$\begin{aligned} \frac{\partial}{\partial x} u(0,t) &= e^{2t} + 1 \\ &= 2 + \frac{t^{\alpha}}{\Gamma(\alpha+1)} f'(0) + \frac{t^{2\alpha}}{\Gamma(2\alpha+1)}\left(8 + 2f'''(0)\right) \\ &\quad + \frac{t^{3\alpha}}{\Gamma(3\alpha+1)}\left(4f^{(5)}(0)\right) + \cdots . \end{aligned}$$

Hence, this yields

$$f^{(2n+1)}(0;\alpha) = \begin{cases} \frac{2^{\alpha n+1} - 2^{n+2}}{2^n}, & n = 1, 3, 5, \ldots, \\ \frac{2^{\alpha n+1}}{2^n}, & n = 0, 2, 4, \ldots . \end{cases} \tag{6.7}$$

Combining (6.6) and (6.7) leads to the Taylor expansion of $f(x)$ *at* $x = 0$ *as*

$$\begin{aligned} f(x;\alpha) &= \sum_{n=0}^{\infty} f^{(2n)}(0;\alpha) \frac{x^{2n}}{(2n)!} + \sum_{\substack{n=1 \\ n\ odd}}^{\infty} f^{(2n+1)}(0;\alpha) \frac{x^{2n+1}}{(2n+1)!} \\ &\quad + \sum_{\substack{n=0 \\ n\ even}}^{\infty} f^{(2n+1)}(0;\alpha) \frac{x^{2n+1}}{(2n+1)!} \\ &= -2\cosh(x) + 2^{\alpha}\cosh\left(2^{\frac{1}{2}(-1+\alpha)} x\right) \\ &\quad + 2\sin(x) - 2\sinh(x) + 2^{\frac{1+\alpha}{2}} \sinh\left(2^{\frac{1}{2}(-1+\alpha)} x\right). \end{aligned}$$

Substituting $f(x;\alpha)$ *into Eq (6.5) enables us to obtain the solution* $u(x,t;\alpha)$ *as*

$$
\begin{aligned}
u(x,t;\alpha) = {} & e^x E_{\alpha,1}(2t^\alpha) + \sin(x) E_{\alpha,1}(-2t^\alpha) \\
& + \Big(-2\cosh(x) + 2^\alpha \cosh(2^{\frac{1}{2}(-1+\alpha)}x) \\
& + 2\sin(x) - 2\sinh(x) + 2^{\frac{1+\alpha}{2}} \sinh(2^{\frac{1}{2}(-1+\alpha)}x)\Big) \frac{t^\alpha}{\Gamma(\alpha+1)} \\
& + 2\Big(-2\cosh(x) + 2^{-1+2\alpha} \cosh(2^{\frac{1}{2}(-1+\alpha)}x) \\
& - 2\sin(x) - 2\sinh(x) + 2^{-\frac{1}{2}+\frac{3\alpha}{2}} \sinh(2^{\frac{1}{2}(-1+\alpha)}x)\Big) \frac{t^{2\alpha}}{\Gamma(2\alpha+1)} \\
& + 4\Big(-2\cosh(x) + 2^{-2+3\alpha} \cosh(2^{\frac{1}{2}(-1+\alpha)}x) \\
& + 2\sin(x) - 2\sinh(x) + 2^{-\frac{3}{2}+\frac{5\alpha}{2}} \sinh(2^{\frac{1}{2}(-1+\alpha)}x)\Big) \frac{t^{3\alpha}}{\Gamma(3\alpha+1)} \\
& + \cdots .
\end{aligned}
$$

The derivative of order $(2n-2)$ of $f(x)$ can be rearranged for $n \geq 1$ as

$$
\begin{aligned}
f^{(2n-2)}(x;\alpha) = {} & -2\cosh(x) + 2^{\alpha+(2n-2)k} \cosh(2^k x) \\
& + 2(-1)^{n-1} \sin(x) - 2\sinh(x) \\
& + 2^{\frac{1+\alpha}{2}+(2n-2)k} \sinh(2^k x),
\end{aligned}
$$

where $k = \frac{\alpha-1}{2}$.

So, it follows that the solution $u(x,t;\alpha)$ can be obtained as

$$
\begin{aligned}
u(x,t;\alpha) = {} & e^x E_{\alpha,1}(2t^\alpha) + \sin(x) E_{\alpha,1}(-2t^\alpha) \\
& + \sum_{n=1}^{\infty} 2^{n-1} f^{(2n-2)}(x) \frac{t^{n\alpha}}{\Gamma(n\alpha+1)},
\end{aligned}
$$

which rapidly converges to

$$
u(x,t;\alpha) = e^x E_{\alpha,1}(2t^\alpha) + \sin(x).
$$

Example 2. *Consider the fractional inverse source problem*

$$
\mathcal{D}_t^\alpha u(x,t) = \frac{1}{2}x^2 u_{xx}(x,t) + f(t), \qquad x > 0,\ 0 < \alpha \leq 1,\ t > 0, \tag{6.8}
$$

$$
u(x,0) = x^2 + \frac{1}{2}, \tag{6.9}
$$

$$
u(0,t) = \frac{e^{2t}}{2}, \tag{6.10}
$$

$$
u_x(0,t) = 0. \tag{6.11}
$$

Application of the Laplace and inverse Laplace transform to Eq (6.8) successively yields

$$
u(x,t) = \mathcal{L}^{-1}\left[\frac{1}{s}\left(x^2 + \frac{1}{2}\right)\right] + \mathcal{L}^{-1}\left[\frac{1}{s^\alpha}\mathcal{L}\left[\frac{1}{2}x^2 u_{xx}(x,t) + f(t)\right](s)\right].
$$

$u_0(x,t)$ is computed as

$$u_0(x,t) = x^2 + \frac{1}{2}.$$

$u_1(x,t;\alpha)$, $u_2(x,t;\alpha)$, and $u_3(x,t;\alpha)$ are determined by DJM as

$$\begin{aligned} u_1(x,t;\alpha) &= \frac{t^\alpha}{\Gamma(\alpha+1)}x^2 + \frac{t^{\alpha-1}}{\Gamma(\alpha)} * f(t), \\ u_2(x,t;\alpha) &= x^2\frac{t^{2\alpha}}{\Gamma(2\alpha+1)}, \\ u_3(x,t;\alpha) &= x^2\frac{t^{3\alpha}}{\Gamma(3\alpha+1)}. \end{aligned}$$

The truncated solution for $u(x,t;\alpha)$ is acquired as

$$\begin{aligned} u(x,t;\alpha) &= \frac{1}{2} + \frac{t^{\alpha-1}}{\Gamma(\alpha)} * f(t) \\ &\quad + x^2\left(1 + \frac{t^\alpha}{\Gamma(\alpha+1)} + \frac{t^{2\alpha}}{\Gamma(2\alpha+1)} + \frac{t^{3\alpha}}{\Gamma(3\alpha+1)} + \cdots\right) \\ &= \frac{1}{2} + \frac{t^{\alpha-1}}{\Gamma(\alpha)} * f(t) + x^2 E_{\alpha,1}(t^\alpha). \end{aligned}$$

Employing the boundary condition (6.10) yields

$$u(0,t) = \frac{e^{2t}}{2} = \frac{1}{2} + \frac{t^{\alpha-1}}{\Gamma(\alpha)} * f(t;\alpha). \tag{6.12}$$

In order to recover the unknown source function from the boundary condition (6.10), we apply the Laplace transform to Eq (6.12), which yields

$$\mathcal{L}[f(t;\alpha)] = s^\alpha\left(\frac{1}{2(-2+s)} - \frac{1}{2s}\right).$$

Application of the inverse Laplace transformation enables us to establish the unknown source function as follows:

$$f(t;\alpha) = -\frac{t^{-\alpha}}{2\Gamma(1-\alpha)} + \frac{2^{-1+\alpha}e^{2t}\left(\Gamma(-\alpha) - \Gamma(-\alpha,2t)\right)}{\Gamma(-\alpha)}.$$

Notice that the other boundary condition $u_x(0,t) = 0$ is not used in the determination of an unknown function of time unlike the unknown function of a spatial variable. This is a great advantage of the proposed method, which provides significant contribution in this respect. Moreover, in the numerical solutions of various inverse problems, the developed methods use overmeasured data in addition to initial and boundary conditions, while this method provides an analytical solution of the inverse problem without any overmeasured data.

Substituting the obtained unknown source function into the solution of problems (6.8)–(6.11) leads to

$$u(x,t;\alpha) = \frac{1}{2} + \left(\frac{t^{\alpha-1}}{\Gamma(\alpha)} * \left(-\frac{t^{-\alpha}}{2\Gamma(1-\alpha)} + \frac{2^{-1+\alpha}e^{2t}\left(\Gamma(-\alpha) - \Gamma(-\alpha,2t)\right)}{\Gamma(-\alpha)}\right)\right) + x^2 E_{\alpha,1}(t^\alpha).$$

In the computation of the convolution in the solution, we employ Laplace and inverse Laplace transformations, which give rise to

$$u(x,t;\alpha) = \frac{1}{2} + \frac{1}{2}(-1 + e^{2t}) + x^2 E_{\alpha,1}(t^\alpha) = \frac{e^{2t}}{2} + x^2 E_{\alpha,1}(t^\alpha).$$

For $\alpha = 1$, we get

$$u(x,t) = \frac{e^{2t}}{2} + x^2 e^t,$$

which is the analytical solution of the classical diffusion problem under consideration.

7. Results and discussion

As can be seen from Figure 4 and Table 1, the behavior of the solution is very similar to the behavior of the exact solution which represents classical diffusion as α tends to 1. Therefore, we conclude that the memory effect on the solution vanishes as α tends to 1. Moreover, as α decreases, the solution increases faster than the exact solution as a result of the order of the fractional derivative. Another observation of the solution from Figure 4 and Table 1 is that exact solution grows exponentially like classical diffusion behavior, while the growth rate of fractional solutions increases as α decreases and t increases. Moreover, strong memory effect can be observed from solution lags. The Mittag-Leffler function $E_{\alpha,1}(2t^\alpha)$ in the solution of Example 1 initially provides rapid growth but later decelerating growth for $\alpha < 1$. Thus, fractional solutions stay above the exact solution with more bending. Furthermore, the Mittag-Leffler function $E_{\alpha,1}(-2t^\alpha)$ acts as a damping function and gives rise to oscillation in the solution. This analysis leads to the following conclusion that the solutions in Example 1 have memory effect and faster responses for $\alpha < 1$. These outcomes demonstrate that this problem plays a significant role in modeling various complex processes.

Table 1. The obtained values of $u(1,t;\alpha)$ for various α values in Example 1.

t	$\alpha = 0.75$	$\alpha = 0.85$	$\alpha = 0.95$	$\alpha = 1$	Exact solution
0	3.55975281	3.55975281	3.55975281	3.55975281	3.55975281
0.25	7.20085958	6.22312378	5.57170704	5.32316006	5.32316006
0.5	13.27516844	10.55560534	8.85673664	8.23052708	8.23052708
0.75	24.54361850	18.10843423	14.35350208	13.02396495	13.02396495
1	45.63158079	31.36226951	23.57539780	20.92700791	20.92700791

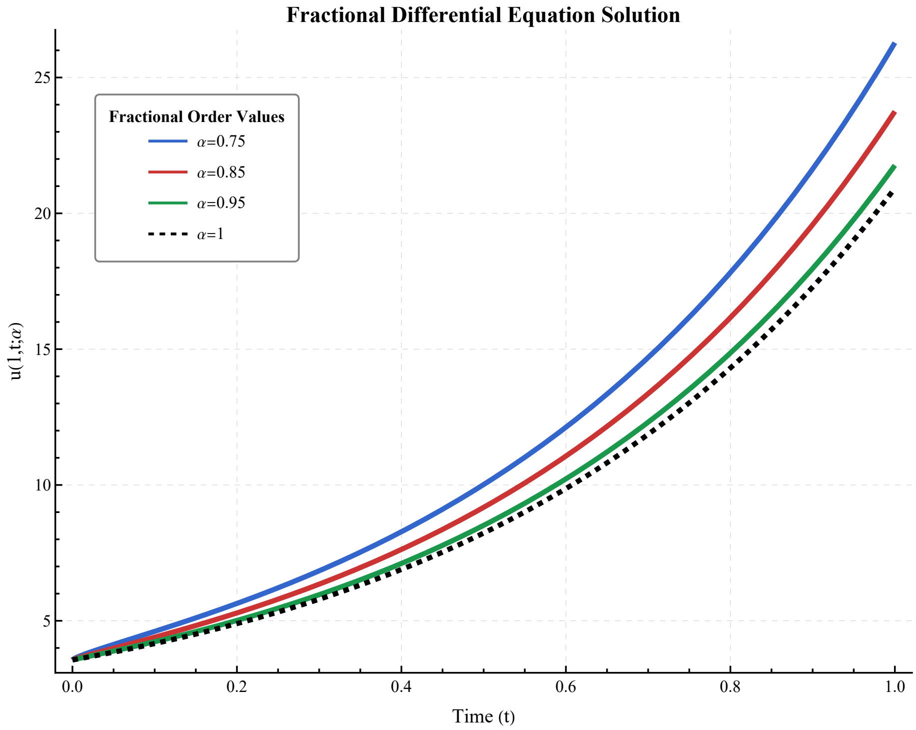

Figure 4. The 2D graphs of fractional and exact solutions to Example 1 for various values of α.

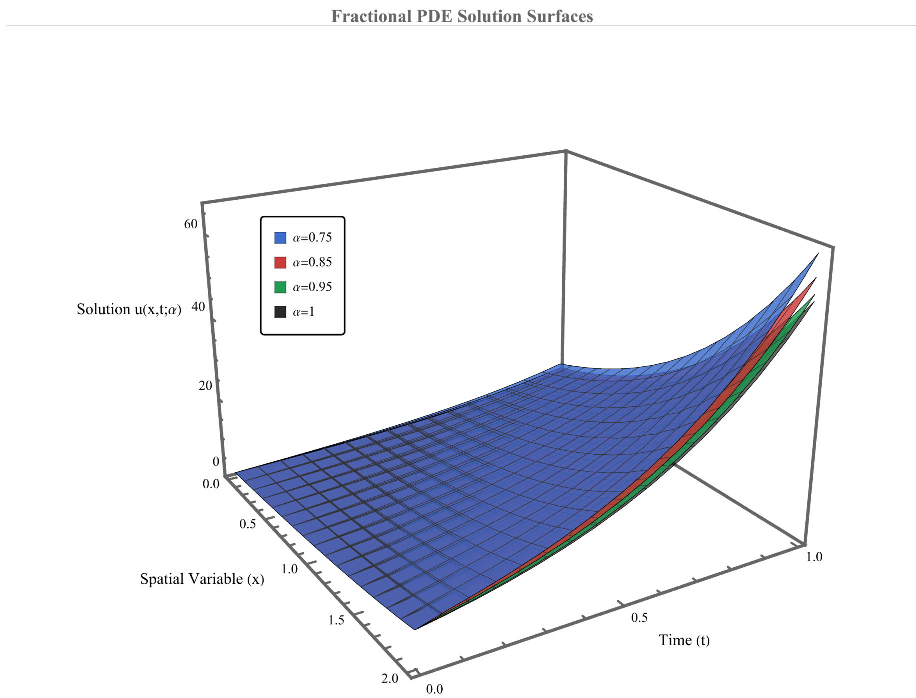

Figure 5. The 3D graphs of fractional and exact solutions to Example 1 for various values of α.

It can be observed from Figure 5 that as the distance increases the fractional and exact solutions also increase, which models an increasing effect of the distance. Moreover, the fractional solutions demonstrate oscillatory behavior along the time axis. As α decreases, the amplitude of the solution increases as a result of memory effect and faster diffusion. This graph visually verifies that fractional diffusion for $\alpha < 1$ is a regularized form of classical diffusion as a result of memory-dependent smoothing and faster energy propagation. Such behavior is generally observed in complex systems.

It is clear from Figure 6, Table 2, and the expression of the source function $f(x;\alpha)$ in Example 1 that the existence of the hyperbolic functions $\cosh(x)$, $\cosh\left(2^{\frac{1}{2}(-1+\alpha)}x\right)$, $\sinh(x)$, and $\sinh\left(2^{\frac{1}{2}(-1+\alpha)}x\right)$ in the source function leads to exponential growth as α and x increase. Moreover, the variation of the source function gets slower as α decreases. Furthermore, the hyperbolic functions distort or modulate the periodic behavior of the source function for $\alpha < 1$. As a result of the nonlocal smoothing effect of the fractional derivative, the source function $f(x;\alpha)$ exhibits damped oscillations which can be noticed from decaying amplitude.

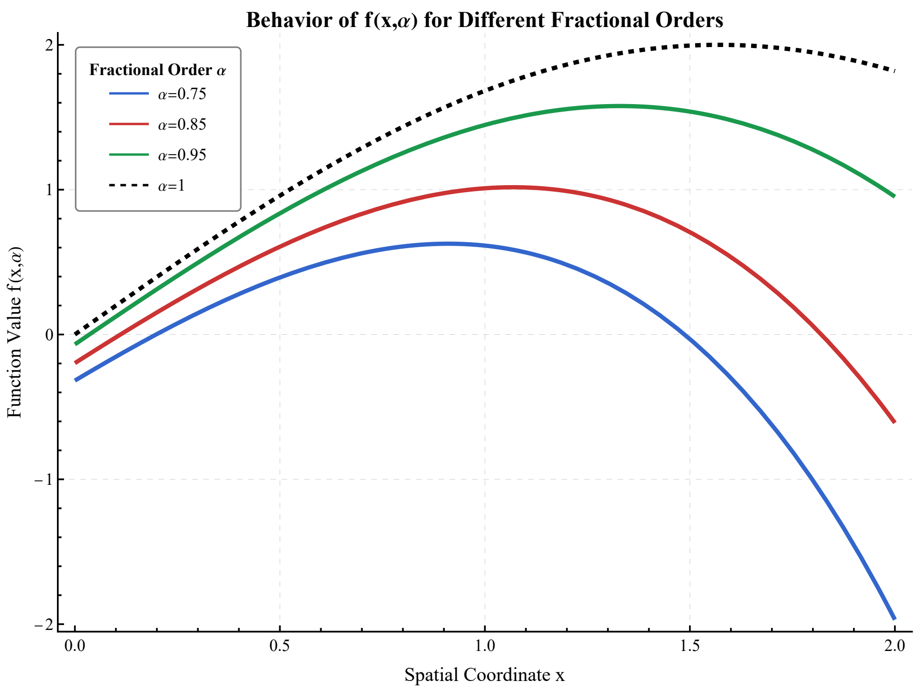

Figure 6. 2D graphs of source function $f(x;\alpha)$ in Example 1 for various values of α.

Table 2. The obtained values of $f(x;\alpha)$ for various α values in Example 1.

x	$\alpha = 0.75$	$\alpha = 0.85$	$\alpha = 0.95$	$\alpha = 1$	Exact solution
0	-0.31820717	-0.19749907	-0.06812734	0	0
0.5	0.39376718	0.60629167	0.83655621	0.95885108	0.95885108
1	0.61384406	1.00971520	1.44710315	1.68294197	1.68294197
1.5	-0.03147090	0.70694552	1.53928358	1.99498997	1.99498997
2	-1.96911402	-0.61012214	0.95124628	1.81859485	1.81859485

Table 3. Convergence analysis for $u(1, t; \alpha)$ in Example 1 ($0 < t < 1$).

Iteration number (n)	α values 0.75	0.85	0.95	1.00
2	9.2979172907	3.8381707966	0.7748827388	0.2891694032
3	10.4218748278	4.6106658901	1.2905237892	0.1358122471
5	10.1251105139	4.3822040703	1.1402772789	0.0163029682
7	9.9742627901	4.3180866011	1.1164994854	0.0010677460
9	9.9311500149	4.3080424590	1.1144681075	0.0000440724
11	9.9227446044	4.3069990673	1.1143570919	$1.2521631090 \times 10^{-6}$
13	9.9215223282	4.3069205793	1.1143528418	$2.5992434171 \times 10^{-8}$
15	9.9213825546	4.3069160613	1.1143527209	$4.1155833829 \times 10^{-10}$

It is clear from Table 3 that as the iteration number n and the order of the time fractional derivative α increases, the solution $u\left(\frac{\pi}{4}, t; \alpha\right)$ gets closer to the exact solution. It can be observed from Figure 5 that the same thing happens for all values of x, which leads to the convergence of the truncated solution to the exact solution.

For the rate of the convergence in terms of iteration number n, we have the following inequality:

$$||u_n - u_{\text{exact}}|| \leq C\frac{t^{(n+1)\alpha}}{\Gamma((n+1)\alpha + 1)},$$

where C is a constant depending on $||f^{(2n)}(x)||_\infty$.

It is obvious from Table 4 that as the iteration number n increases, the values converge to the source function $f(x; \alpha)$ for various values of α.

Table 4. Convergence analysis for $f(x; \alpha)$ in Example 1 ($0 < x < 2$).

Iteration number (n)	α values 0.75	0.85	0.95	1.00
2	0.66804239	0.45533975	0.89404885	1.22095879
3	2.21145852	1.46775762	0.64268219	0.20995876
5	2.32732525	1.47493328	0.51259385	0.01766724
7	2.38124959	1.51674137	0.53823128	0.00088611
9	2.38301577	1.51776155	0.53818648	0.00002956
11	2.38314039	1.51785786	0.53823930	$7.03572498 \times 10^{-7}$
13	2.38314273	1.51785945	0.53823967	$1.25004559 \times 10^{-8}$
15	2.38314279	1.51785950	0.53823970	$1.72878043 \times 10^{-10}$

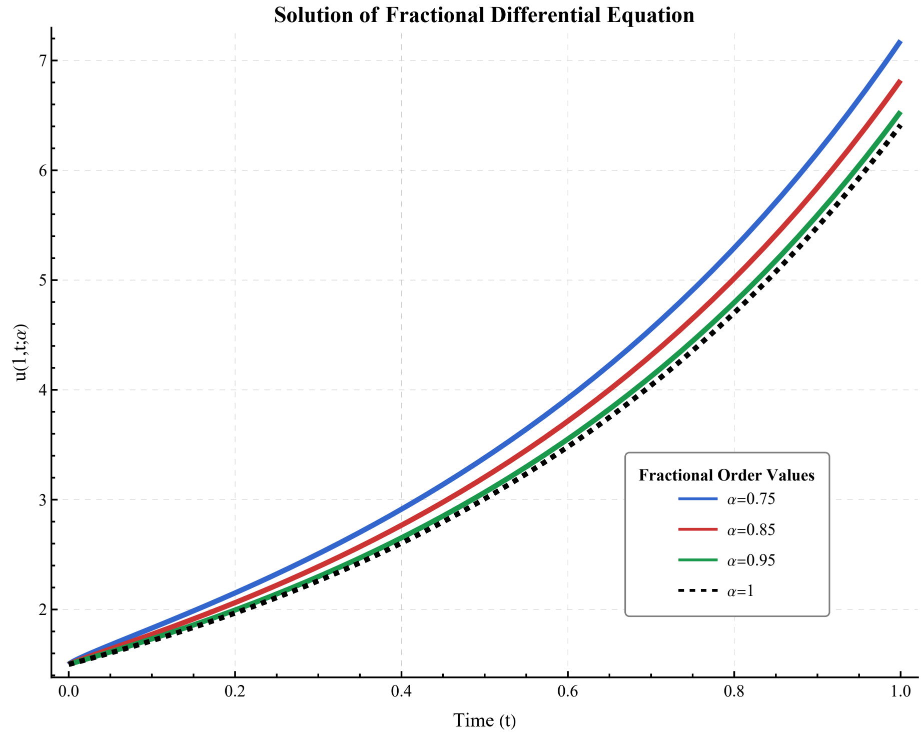

Figure 7. The 2D graphs of fractional and exact solutions to Example 2 for various values of α.

Table 5. The obtained values of $u(1, t; \alpha)$ for various α values in Example 2.

t	$\alpha = 0.75$	$\alpha = 0.85$	$\alpha = 0.95$	$\alpha = 1$	Exact solution
0	1.50000000	1.50000000	1.50000000	1.50000000	1.50000000
0.25	2.32339614	2.22044701	2.14125957	2.10838605	2.10838605
0.5	3.38086091	3.20476411	3.06639662	3.00786218	3.00786218
0.75	4.90923408	4.65001207	4.44504723	4.35784455	4.35784455
1	7.18039427	6.82002241	6.53450882	6.41280987	6.41280987

Figure 7 and Table 5 clearly demonstrate that the behavior of the fractional solution closely approximates the exact solution, which characterizes classical diffusion, as the parameter α approaches 1. This indicates that the memory effects inherent in the fractional model diminish in the limit $\alpha \to 1$. Furthermore, as α decreases, the solution exhibits a more rapid growth compared to the exact solution, highlighting the influence of the fractional order. Additionally, it is observed that while the exact solution grows exponentially-consistent with classical diffusion, the growth rate of the fractional solutions becomes increasingly pronounced with decreasing α and increasing time t. Another observation of the solution from Figure 7 and Table 5 that exact solution grows exponentially like classical diffusion behavior while growth rate of fractional solutions increases as α decreases and t increases. Moreover, strong memory effect can be observed from solution lags. These outcomes give rise to the following conclusion that the solutions in Example 2 have memory effect and faster responses for $\alpha < 1$.

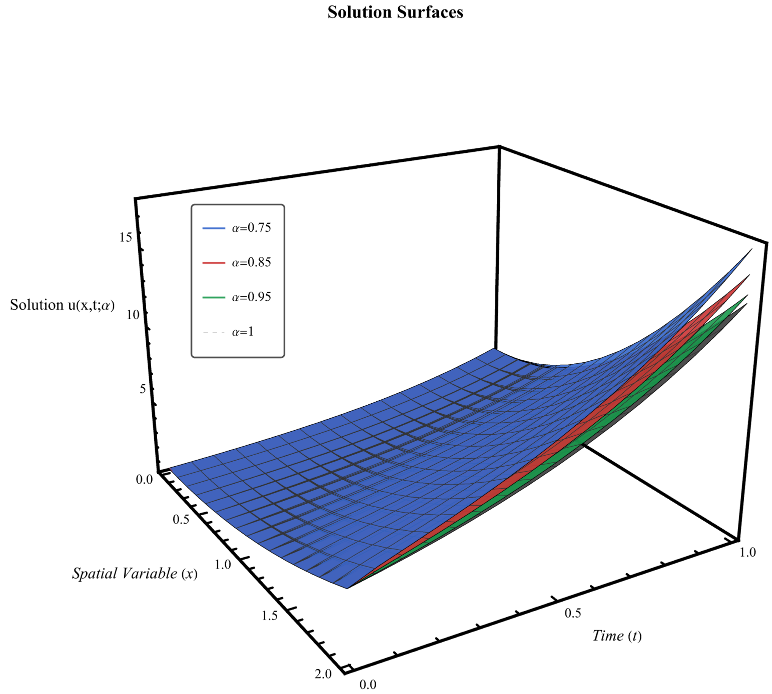

Figure 8. The 3D graphs of fractional and exact solutions to Example 2 for various values of α.

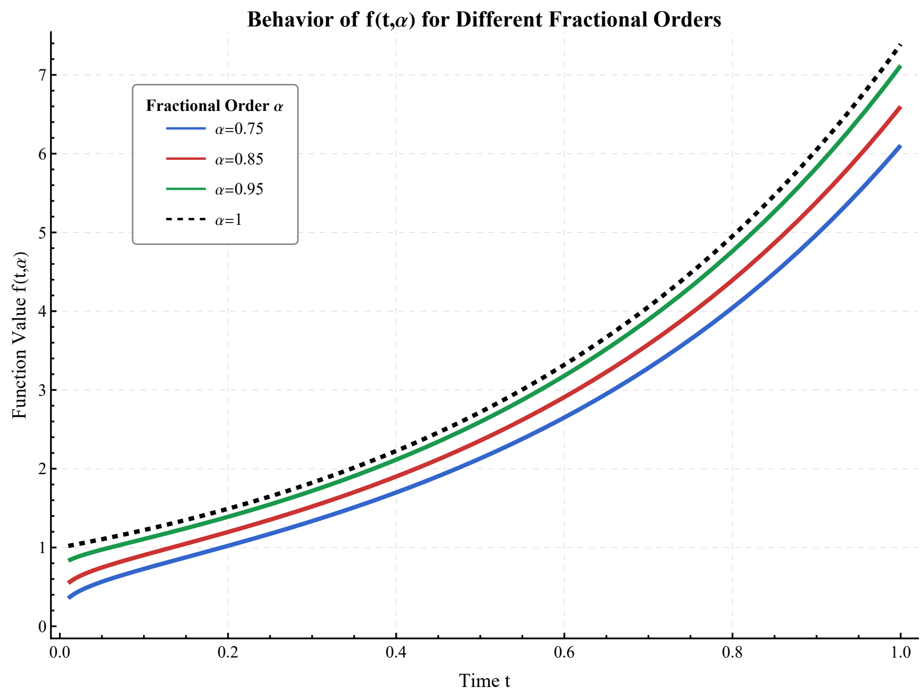

Figure 9. 2D graphs of source function $f(t;\alpha)$ in Example 2 for various values of α.

Table 6. The obtained values of $f(t;\alpha)$ for various α values in Example 2.

t	$\alpha = 0.75$	$\alpha = 0.85$	$\alpha = 0.95$	$\alpha = 1$	Exact solution
0.01	0.35451433	0.54658388	0.83164184	1.02020134	1.02020134
0.25	1.17357197	1.35289564	1.54688097	1.64872127	1.64872127
0.5	2.13053977	2.35733728	2.59542966	2.71828183	2.71828183
0.75	3.64270185	3.96630697	4.30592836	4.48168907	4.48168907
1	6.10602535	6.59866166	7.11852550	7.38905609	7.38905609

Figure 8 illustrates that both the fractional and exact solutions exhibit an increasing trend with respect to spatial position, indicating an amplifying effect associated with distance. Additionally, the fractional solutions display a pronounced oscillatory pattern along the temporal axis, reflecting dynamic temporal variations. As α decreases, the amplitude of the solution increases as a result of memory effect and faster diffusion. This graph visually confirms that fractional diffusion for $\alpha < 1$ is the regularized form of classical diffusion as a result of memory-dependent smoothing and faster energy propagation. Such behavior is generally observed in complex systems.

Figure 9 and Table 6 illustrate that the source function for $\alpha = 1$ displays exponential growth, while it displays slower long-term growth for $\alpha < 1$ as a result of memory effect and initial singularity. This source function can model external source functions in the modeling of reactive transport systems, heat transfer, and viscoelasticity. Furthermore, the variation of the source function gets slower as α decreases. As a result of the nonlocal smoothing effect of the fractional derivative, the source function $f(t;\alpha)$ exhibits decaying amplitude as α decreases.

It is clear from Table 7 that as the iteration number n and the order of the time fractional derivative α increases, the solution $u(1, 0.5;\alpha)$ gets closer to the exact solution. It can be observed from Figure 8 that the same thing happens for all values of x and t, which leads to the convergence of the truncated solution to the exact solution.

Table 7. Convergence analysis for $u(1, 0.5;\alpha)$ in Example 2.

Iteration number (n)	$\boldsymbol{\alpha}$ values 0.75	0.85	0.95	1.00
2	1.47265169	1.62924898	1.77204835	0.02372127
3	1.55511654	1.67785211	1.79986696	0.00288794
5	1.58043104	1.68869071	1.80436345	0.00002335
7	1.58141751	1.68892006	1.80441395	$1.02545366 \times 10^{-7}$
9	1.58144225	1.68892298	1.80441426	$2.81876744 \times 10^{-10}$
11	1.58144269	1.68892300	1.80441426	$5.30242517 \times 10^{-13}$
13	1.58144269	1.68892300	1.80441426	$8.88178420 \times 10^{-16}$
15	1.58144269	1.68892300	1.80441426	0.00000000

For the rate of the convergence in terms of iteration number n, we have the following inequality:

$$\|u_n - u_{\text{exact}}\| \leq C \frac{t^{(n+1)\alpha}}{\Gamma((n+1)\alpha + 1)},$$

where C is a constant depending on x^2 and t.

It can be observed from Figure 10 that the truncated solutions at $x = 1$ and $\alpha = 0.75$ get closer to the analytical solution as n increases, which confirms the convergence of the truncated solutions to the analytical solution.

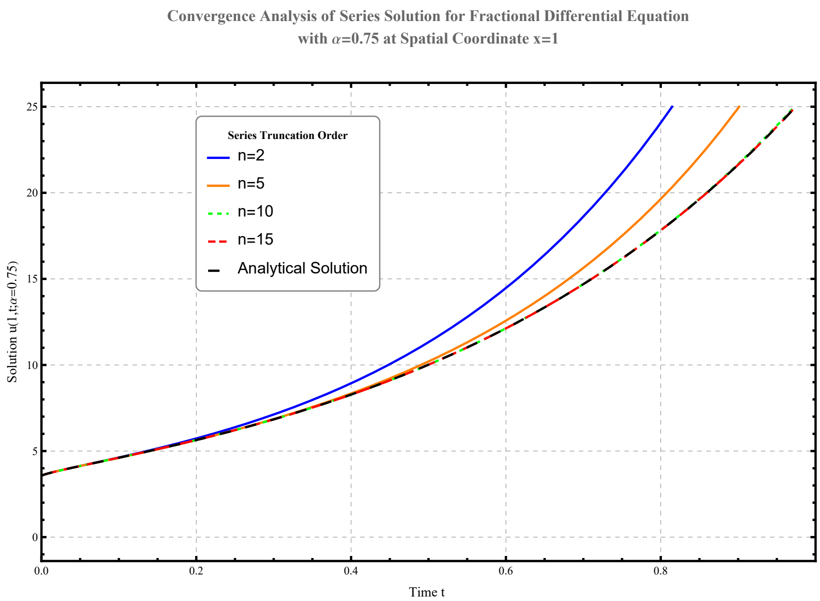

Figure 10. The graphs of truncated solutions $u_n(1, t; 0.75)$ for various values of n for Example 1.

8. Conclusions

In the considered problem, there is no overmeasured data; instead, initial and mixed boundary conditions are prescribed. The source function depends either on time t or spatial variable x. We aim to determine both the source function and the solution of the problem analytically in terms of an arbitrary order of the fractional derivative.

First, by applying the Laplace and inverse Laplace transforms, the fractional partial differential equation is converted into an algebraic equation. Second, the Daftardar-Gejji and Jafari method (DJM) is employed to obtain the solution of the direct problem, which includes the unknown source term. Finally, by utilizing the mixed boundary conditions, we analytically determine the source function that depends solely on the spatial variable x, or, alternatively, by employing the properties of the Laplace transform of convolutions along with the boundary data, we derive the time-dependent source function.

The proposed method is straightforward, easy to implement, and provides an explicit analytical solution in terms of the desired fractional order. We also present theoretical results that establish the existence, uniqueness, and stability of the solution. To demonstrate its applicability and reliability, two illustrative examples are provided along with their corresponding graphical representations and tables.

In a future study, we will combined various integral transforms with a powerful iterative method to develop new approaches to establish truncated and analytical solutions for various fractional inverse problems.

Use of AI tools declaration

The authors declare they have not used Artificial Intelligence (AI) tools in the creation of this article.

Acknowledgments

The author gratefully acknowledges the helpful comments and suggestions of the reviewers, which have improved the presentation. I would like to thank Kocaeli University Scientific Research Projects Coordination Unit for the opportunities provided (4692).

Conflict of interest

The authors declare there are no conflicts of interest.

References

1. K. B. Oldham, J. Spanier, *The Fractional Calculus*, Academic Press, New York, 1974.
2. I. Podlubny, *Fractional Differential Equations*, Academic Press, New York, 1999. https://doi.org/10.1016/S0076-5392(99)X8001-5
3. R. Hilfer, *Applications of Fractional Calculus in Physics*, World Scientific, Germany, 2000. https://doi.org/10.1142/3779
4. F. Mainardi, *Fractional Calculus and Waves in Linear Viscoelasticity: An Introduction to Mathematical Models*, World Scientific, Bologna, 2010. https://doi.org/10.1142/p614
5. Z. Achouri, N. E. Amroun, A. Benaissa, The Euler–Bernoulli beam equation with boundary dissipation of fractional derivative type, *Math. Methods Appl. Sci.*, **40** (2017), 3837–3854. https://doi.org/10.1002/mma.4267
6. M. M. AlBaidani, A. H. Ganie, F. Aljuaydi, A. Khan, Application of analytical techniques for solving fractional physical models arising in applied sciences, *Fractal Fract.*, **7** (2023), 584. https://doi.org/10.3390/fractalfract7080584
7. K. Chalambari, H. Ebrahimi, Z. Ayati, Stability and convergence of a new hybrid method for fractional partial differential equations, *Math. Sci.*, **18** (2024), 367–386. https://doi.org/10.1007/s40096-022-00506-9
8. T. Eriqat, M. N. Oqielat, Z. Al-Zhour, G. S. Khammash, A. El-Ajou, H. Alrabaiah, Exact and numerical solutions of higher-order fractional partial differential equations: A new analytical method and some applications, *Pramana*, **96** (2022), 207. https://doi.org/10.1007/s12043-022-02446-4
9. N. A. Shah, I. Dassios, E. R. El-Zahar, J. D. Chung, An efficient technique of fractional-order physical models involving ρ-Laplace transform, *Mathematics*, **10** (2022), 816. https://doi.org/10.3390/math10050816
10. A. Ghafoor, N. Khan, M. Hussain, R. Ullah, A hybrid collocation method for the computational study of multi-term time fractional partial differential equations, *Comput. Math. Appl.*, **128** (2022), 130–144. https://doi.org/10.1016/j.camwa.2022.10.005

11. B. K. Turmetov, B. J. Kadirkulov, On the solvability of an initial-boundary value problem for a fractional heat equation with involution, *Lobachevskii J. Math.*, **43** (2022), 249–262. https://doi.org/10.1134/S1995080222040217

12. A. A. Kilbas, H. M. Srivastava, J. J. Trujillo, *Theory and Applications of Fractional Differential Equations*, Elsevier, 2006. https://doi.org/10.1016/S0304-0208(06)X8001-5

13. Y. Li, Y. Q. Chen, I. Podlubny, Stability of fractional-order nonlinear dynamic systems: Lyapunov direct method and generalized Mittag–Leffler stability, *Comput. Math. Appl.*, **59** (2010), 1810–1821. https://doi.org/10.1016/j.camwa.2009.08.019

14. I. Ali, H. Khan, R. Shah, D. Baleanu, P. Kumam, M. Arif, Fractional view analysis of acoustic wave equations, using fractional-order differential equations, *Appl. Sci.*, **10** (2020), 610. https://doi.org/10.3390/app10020610

15. R. M. Jena, S. Chakraverty, On the solution of time-fractional coupled system of partial differential equations, *SN Appl. Sci.*, **1** (2019), 1655. https://doi.org/10.1007/s42452-019-1676-9

16. J. Ren, Z. Z. Sun, W. Dai, New approximations for solving the Caputo-type fractional partial differential equations, *Appl. Math. Modell.*, **40** (2016), 2625–2636. https://doi.org/10.1016/j.apm.2015.10.011

17. R. Sahadevan, P. Prakash, Exact solution of certain time fractional nonlinear partial differential equations, *Nonlinear Dyn.*, **85** (2016), 659–673. https://doi.org/10.1007/s11071-016-2714-4

18. H. Zhang, M. Nadeem, A. Rauf, Z. G. Hui, A novel approach for the analytical solution of nonlinear time-fractional differential equations, *Int. J. Numer. Methods Heat Fluid Flow*, **31** (2021), 1069–1084. https://doi.org/10.1108/HFF-02-2020-0077

19. X. B. Yin, S. Kumar, D. Kumar, A modified homotopy analysis method for solution of fractional wave equations, *Adv. Mech. Eng.*, **7** (2015), 1–8. https://doi.org/10.1177/1687814015620330

20. J. Weng, X. Liu, Y. Zhou, J. Wang, An explicit wavelet method for solution of nonlinear fractional wave equations, *Mathematics*, **10** (2022), 4011. https://doi.org/10.3390/math10214011

21. S. Kukla, U. Siedlecka, On solutions of the initial value problem for the three-term fractional differential equation with Caputo derivatives, *Symmetry*, **12** (2020), 1355. https://doi.org/10.3390/sym12081355

22. V. Daftardar-Gejji, H. Jafari, An iterative method for solving nonlinear functional equations, *J. Math. Anal. Appl.*, **316** (2006), 753–763. https://doi.org/10.1016/j.jmaa.2005.05.009

23. V. Daftardar-Gejji, S. Bhalekar, Chaos in fractional ordered Liu system, *Comput. Math. Appl.*, **59** (2010), 1117–1127. https://doi.org/10.1016/j.camwa.2009.07.003

24. L. Ali, S. Islam, T. Gul, I. S. Amiri, Solution of nonlinear problems by a new analytical technique using Daftardar-Gejji and Jafari polynomials, *Adv. Mech. Eng.*, **11** (2019), 1–10. https://doi.org/10.1177/1687814019896962

25. S. Cetinkaya, A. Demir, A new approach for the fractional Rosenau–Hyman problem by ARA transform, *Math. Methods Appl. Sci.*, **48** (2025), 10970–10977. https://doi.org/10.1002/mma.10934

26. S. Cetinkaya, A. Demir, On the solution of time fractional initial value problem by a new method with ARA transform, *J. Intell. Fuzzy Syst.*, **44** (2022), 2693–2701. https://doi.org/10.3233/JIFS-223237

27. H. K. Sevindir, S. Cetinkaya, A. Demir, On effects of a new method for fractional initial value problems, *Adv. Math. Phys.*, **2021** (2021), 606442. https://doi.org/10.1155/2021/7606442

28. F. Mihoubi, B. Nouiri, An inverse time-dependent source problem for a time-fractional diffusion equation with nonlocal boundary conditions, *Miskolc Math. Notes*, **25** (2024), 873–889. https://doi.org/10.18514/MMN.2024.4495

29. B. Derbissaly, M. Sadybekov, Inverse source problem for multi-term time-fractional diffusion equation with nonlocal boundary conditions, *AIMS Math.*, **9** (2024), 9969–9988. https://doi.org/10.3934/math.2024488

30. M. Nouar, C. Abdeledjalil, O. M. Alsalhi, H. O. Sidi, Inverse problem of identifying a time-dependent source term in a fractional degenerate semi-linear parabolic equation, *Mathematics*, **9** (2025), 1486. https://doi.org/10.3390/math13091486

31. M. Abdelwahed, M. BenSaleh, N. Chorfi, M. Hassine, An inverse problem study related to a fractional diffusion equation, *J. Math. Anal. Appl.*, **512** (2022), 126145. https://doi.org/10.1016/j.jmaa.2022.126145

32. M. A. Bayrak, A. Demir, On the inverse problem of time dependent coefficient in a time fractional diffusion problem by sinc wavelet collocation method, *Phys. Scr.*, **99** (2024), 10. https://doi.org/10.1088/1402-4896/ad753a

33. M. A. Bayrak, A. Demir, On the inverse problem of time-dependent coefficient in a time fractional diffusion problem by newly defined Monic Laquerre wavelets, *J. Comput. Nonlinear Dyn.*, **18** (2023), 111003. https://doi.org/10.1115/1.4063337

34. J. R. Cannon, The solution of the heat conduction subject to the specification of energy, *Quart. Appl. Math.*, **21** (1963), 155–160. https://doi.org/10.1090/qam/160437

35. J. R. Cannon, Determination of an unknown heat source from over-specified boundary data, *SIAM J. Numer. Anal.*, **5** (1968), 275–286. https://doi.org/10.1137/0705024

36. F. F. Dou, C. L. Fu, F. Yang, Identifying an unknown source term in a heat equation, *Inverse Probl. Sci. Eng.*, **17** (2009), 901–913. https://doi.org/10.1080/17415970902916870

37. V. Obukhovskii, G. Petrosyan, M. Soroka, C. F. Wen, On a boundary value problem for Hale type fractional functional-differential inclusions with causal multioperators in a Banach space, *J. Nonlinear Var. Anal.*, **7** (2023), 957–970. https://doi.org/10.23952/jnva.7.2023.6.05

38. M. Kaewsuwan, C. Thaiprayoon, A. Aphithana, J. Kongson, W. Sae-dan, W. Sudsutad, Nonlinear impulsive (ρ_k, ψ_k)-Hilfer fractional pantograph integro-differential equations under nonlocal integral boundary conditions, *J. Nonlinear Funct. Anal.*, **2024** (2024), 10. https://doi.org/10.23952/jnfa.2024.10

39. G. Özkum, A. Demir, S. Erman, K. Esra, B. Özgür, On the inverse problem of the fractional heat-like partial differential equations: Determination of the source function, *Adv. Math. Phys.*, **2013** (2013), 476154. https://doi.org/10.1155/2013/476154

40. V. Gülkaç, A method of finding source function for inverse diffusion problem with time-fractional derivative, *Adv. Math. Phys.*, **2016** (2016), 6470949. https://doi.org/10.1155/2016/6470949

41. D. A. Benson, S. W. Wheatcraft, M. M. Meerschaert, Application of a fractional advection-dispersion equation, *Water Resour. Res.*, **36** (2000), 1403–1412. https://doi.org/10.1029/2000WR900031

42. Y. Zhang, D. A. Benson, D. M. Reeves, Time and space nonlocalities underlying fractional-derivative models: Distinction and literature review of field applications, *Adv. Water Resour.*, **32** (2009), 561–581 https://doi.org/10.1016/j.advwatres.2009.01.008

43. Á. Cartea, D. del-Castillo-Negrete, Fractional diffusion models of option prices in markets with jumps, *Physica A*, **374** (2007), 749–763. https://doi.org/10.1016/j.physa.2006.08.071

44. E. Scalas, R. Gorenflo, F. Mainardi, Fractional calculus and continuous-time finance, *Physica A*, **284** (2000), 376–384. https://doi.org/10.1016/S0378-4371(00)00255-7

45. J. T. Machado, V. Kiryakova, F. Mainardi, Recent history of fractional calculus, *Commun. Nonlinear Sci. Numer. Simul.*, **16** (2011), 1140–1153. https://doi.org/10.1016/j.cnsns.2010.05.027

46. Y. Povstenko, *Linear Fractional Diffusion-Wave Equation for Scientists and Engineers*, Birkhäuser, New York, 2015. https://doi.org/10.1007/978-3-319-17954-4

47. R. B. Paris, A uniform asymptotic expansion for the incomplete gamma function, *J. Comput. Appl. Math.*, **148** (2002), 323–339. https://doi.org/10.1016/S0377-0427(02)00553-8

48. K. V. Zhukovsky, H. M. Srivastava, Analytical solutions for heat diffusion beyond Fourier law, *Appl. Math. Comput.*, **293** (2017), 423–437. https://doi.org/10.1016/j.amc.2016.08.038

49. X. J. Yang, H. M. Srivastava, D. F. M. Torres, A. Debbouche, General fractional-order anomalous diffusion with non-singular power-law kernel, *Therm. Sci.*, **21** (2017), 1–9. https://doi.org/10.2298/TSCI170610193Y

50. R. Bracewell, *The Fourier Transform And Its Applications*, McGraw-Hill, 2000.

51. Z. M. Odibat, N. T. Shawagfeh, Generalized Taylor's formula, *Appl. Math. Comput.*, **186** (2007), 286–293. https://doi.org/10.1016/j.amc.2006.07.102

52. K. Sakamoto, M. Yamamoto, Initial value/boundary value problems for fractional diffusion-wave equations and applications to some inverse problems, *J. Math. Anal. Appl.*, **382** (2011), 426–447. https://doi.org/10.1016/j.jmaa.2011.04.058